International Science Journal of Engineering & Agriculture
2025; 4(3): 101-113
https://isg-journal.com/isjea
doi: 10.46299/j.isjea.20250403.09
ISSN: 2720-6319

INTERNATIONAL
SCIENCE GROUP

Integrated FEM and neural network-based optimization of the drawing process for variable cross-section forgings

Xiang Zhang
National Aerospace University "Kharkiv Aviation Institute", Ukraine
ORCID 0000-0001-6607-4270

Volodymyr Borysevych
National Aerospace University "Kharkiv Aviation Institute", Ukraine
ORCID 0009-0008-0623-324X

Abstract: This study built a quality prediction model for the drawing process by integrating finite element simulation and neural network technology. It meticulously examines the influence of pivotal process parameters, including temperature, friction, speed, anvil width ratio (b/h), width-height ratio (w/h), and reduction ratio (ξ), on the overall drawing process. To facilitate a precise characterization of the workpiece's shape post-drawing, four key parameters - fullerring coefficient (F), barrelling degree (B), elongation ratio (E), and spread ratio (S) are introduced.The findings reveal that while friction and speed exert minimal influence on the drawing process, factors such as temperature, b/h, w/h, and especially the ξ, hold significant sway. Notably, a single-step reduction of 40% emerges as an optimal choice, with caution advised when exceeding a 50% reduction due to the potential implications on the internal stress state of the workpiece. A neural network framework is employed to analyze collected training data, establishing a high-precision predictive model with a post-training correlation coefficient of 0.973. Model robustness is validated through rigorous testing across three independent datasets. Building on deformation mechanisms of single-step drawing processes, we propose a customized process scheme for variable cross-section forgings. Optimized parameters—temperature (900°C), pressing speed (5 mm/s), friction factor (0.3), ξ=40%, and w/h=1.2—achieve higher efficiency with critical metrics demonstrating exceptional performance: maximum forming force (F=2.84) and minimal barreling distortion (B=5.85%). A single-pass strategy is recommended for production simplification, contingent upon maintaining anvil width exceeding workpiece elongation. These findings provide a robust technical foundation for enhancing production quality and efficiency in variable cross-section forging.

Keywords: Variable cross-section forgings, Drawing process, Neural network, High-precision predictive model, Higher efficiency.

1. Introduction

The elongation process of forgings is indeed a considerably complex material rheological process, wherein the forming quality is jointly influenced by numerous process parameters. This complexity is further exaggerated in the case of intricate forgings with significant axial section variations, as the larger fullerring coefficient not only increases the process difficulty but also elevates the risk of defect generation. Hence, the introduction of new parameters becomes particularly crucial for more accurately depicting the shape changes of components before and after forging. In the domain of forging width spread research, Tomlinson and Stringer [1] took the lead in 1959 by deriving empirical equations to predict spread width and elongation through their investigations, laying a foundation for subsequent studies. Nevertheless, their equations omitted the consideration of friction as an influencing factor and emphasized that the spread ratio (S) was primarily influenced by the shape of the anvil contact surface. As research progressed, other scholars extensively studied the

calculation formulas for the spread ratio (S) and proposed corresponding improvement methods. These scholars integrated additional factors into their prediction models, such as anvil width, workpiece width, the ratio of initial height to width, and material constants, aiming for more accurate predictions of spread ratio variations. They primarily adopted analytical methods and physical experimentation as their research approaches. Currently, several prominent spread ratio prediction models have been put forward[2].

$$S = 0.29 - 0.16\frac{h_1}{h_0} + 0.343\frac{b}{w_0} - 0.048\left(\frac{b}{w_0}\right)^2, \tag{1}$$

$$S = \frac{b}{w_0 + b}, \tag{2}$$

$$S = \frac{b(1.789 - 0.321(h_0 / w_0))}{w_0 + b(1.789 - 0.321(h_0 / w_0))}, \tag{3}$$

$$S = \frac{1}{2}\left(1 - \frac{1}{2\sqrt{3}}\frac{w_0}{b}\tanh\frac{2\sqrt{3}b}{w_0}\right), \tag{4}$$

$$S = 0.74 + 0.095\frac{b}{w_0} + 0.029\frac{b}{h_0} - 0.72\frac{h_1}{h_0}, \tag{5}$$

$$S = 1 - \exp\left(A(b / w_0)^B\right), \tag{6}$$

where: h_1 - The height of the workpiece after forging, mm

h_0 - The height of the workpiece before forging, mm

h - Half the height of the workpiece before forging, mm

b - The anvil width, mm

w_0 - Initial width of workpiece, mm

w_1 - The maximum width of the workpiece, mm

A, B- material constants.

The above formulas fully account for the relationships between process parameters—such as anvil width ratio, workpiece width ratio, and reduction ratio- and the spread ratio. However, considering only the spread ratio as a single-dimensional indicator during the elongation of variable cross-section forgings is far from sufficient. Since the ultimate goal is to obtain an initial workpiece with a large cross-section ratio, the fullering coefficient, which characterizes this ratio, must be introduced as a key factor. Furthermore, due to the inevitable generation of barreling caused by friction on the upper and lower die surfaces, the barrelling degree B must also be considered as an influencing factor. In addition, maxmium elongation ratio, as a constraint on the workpiece's axial dimension, cannot be neglected.

2. Object and subject of research

The focus of this study is to reveal the deformation behavior of the workpiece during the drawing process for variable cross-section forgings, with the goal of determining optimal process parameters, reducing the number of forging steps, and improving both production efficiency and part quality. The research object is an aerospace bracket featuring a large flange structure, with a maximum cross-section ratio of 2.7, as shown in Figure 1a. To enhance forging quality and minimize the number of forging passes, the workpiece must be drawn to better align the axial material distribution with that of the final part, thereby simplifying subsequent forging operations. The initial shape and key dimensions of the workpiece are determined by analyzing the forged part's cross-sectional and diameter profiles, as illustrated in Figures 1b and 1c.

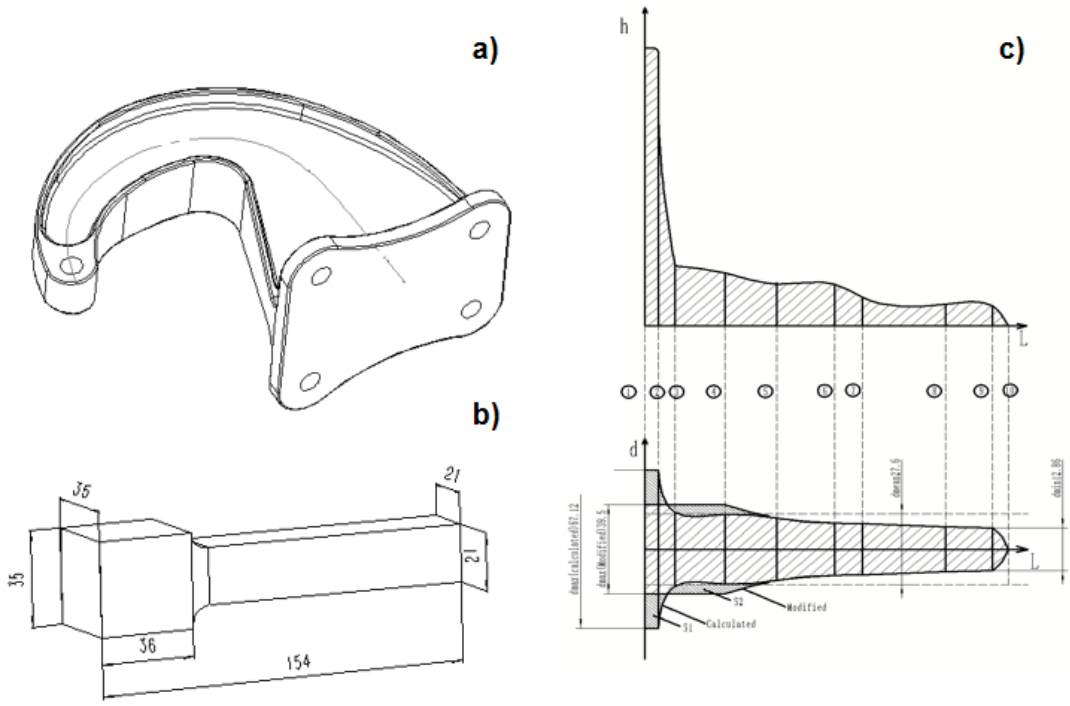

Figure 1. Forging analysis diagram (a - aircraft bracket b - ideal workpiece size after drawing c - cross-sectional and diameter profiles).

3. Target of research

This study aims to establish a clear relationship between key process parameters and the geometric features of drawn forgings, focusing on complex variable cross-section components. Using thermomechanical FEM simulations, a dataset is built to capture deformation under varying conditions. Introduced geometric indicators are used to characterize shape evolution better. A neural network trained on these data enables rapid, accurate prediction of optimal process parameters. This FEM–ANN approach improves forging quality, reduces process steps.

4. Literature analysis

The earliest research on workpiece spread in forging was conducted by Tomlinson and Stringer [5], who developed empirical equations for predicting spread and elongation. These equations did not consider the influence of friction and indicated that the spread coefficient (s) primarily depends on the shape of the anvil contact surface. B. Aksakal and F.H. Osman et al. analyzed spread and elongation during forging using the upper bound method, as illustrated in Fig. 2 [6]. Kudo [7]

proposed a "unit rectangular deformation zone" method for conveniently analyzing complex plane strain problems. Baraya and Johnson [8] employed the upper bound method to investigate the forging process of rod-shaped forgings. By studying triangular velocity zones in three different metals, they proposed solutions for determining force diffusion. These three schemes inherently possess constraints, as they must conform to specific ranges of anvil width ratios.

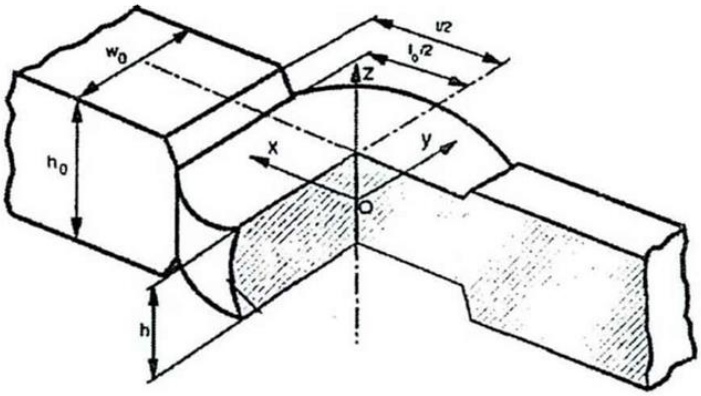

Figure 2. Study on spread and elongation of forgings using the upper bound method.

Safar and Juneja [9] conducted relevant studies on the total required force under consideration of expansion deformation. By performing experiments with rectangular aluminum bars and flat anvils of varying widths, they established the material's rheological laws. Braun et al. [10] addressed issues related to spread and pressure using the upper bound method. In their research, they forged rectangular metal bars using a pair of opposing flat anvils. Kanacri et al. [11] investigated the calculation of stress and displacement during plastic deformation of thin plates by compressing rectangular forgings with two parallel flat plates. Their work demonstrated a rheological curve where spread increases with rising friction coefficient, thereby revising the theory proposed by Hill [2].

Although these researchers using upper bound theory and analytical approximations greatly advanced the understanding of forging mechanics, these methods have notable limitations. They depend on idealized assumptions—such as uniform deformation and rigid-plastic material behavior—that restrict their accuracy under realistic forging conditions. Moreover, they are ill-suited for handling complex geometries and asymmetric deformation, often requiring oversimplification. Additionally, they fail to account for key nonlinearities in material behavior and process parameters, such as temperature dependence, strain rate sensitivity, and variable friction, reducing their applicability to modern, precision forging processes[12]. In contrast, the finite element method (FEM) offers a more advanced and accurate approach to forging analysis by enabling detailed modeling of complex geometries and incorporating realistic material behaviors such as strain hardening, thermal softening, and strain rate sensitivity[13].

Ding[14] conducted an in-depth study on the drawing process of heavy plate forgings by Finite Element Method (FEM). It was found that key elongation process parameters such as reduction ratio , anvil width ratio, width-height ratio, strain rate, friction factor, and initial temperature have significant effects on the forming quality. The results showed that the errors of elongation and widening between each working step did not exceed 3.9%. Therefore, the complex multi-step problem can be simplified into a single-step study, providing a new approach to optimize the elongation process and improve the quality of forgings.

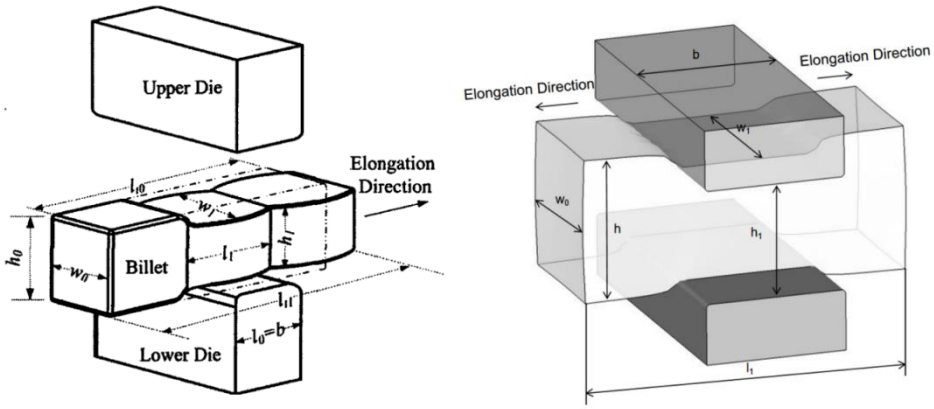

Figure 3. Elongation process (a - Tomlinson and Stringer's model b - this paper 's model).

5. Research methods

This study adopts a hybrid modeling approach that combines the finite element method (FEM) with neural networks. FEM is used to simulate the forming process of variable cross-section forgings under different process parameters, generating high-precision geometric data as training samples for the neural networks. The neural networks is then employed to model complex nonlinear relationships, enabling rapid prediction and multi-objective optimization, thereby significantly reducing the number of simulations and improving efficiency. This method demonstrates strong generalization capability, making it applicable to the process optimization of various forging types and suitable for integration into intelligent manufacturing systems to achieve real-time prediction and process control[15] -[16]. Firstly, 3D thermodynamic coupling finite element model is constructed, focusing on revealing the influences of six key process parameters, namely, temperature (500-900°C), friction factor (0.3-0.7), pressing speed (5-15mm/s), anvil-width ratio (b/h=0.6-1.2), width-height ratio (w/h=0.6-1.2), and reduction ratio (ξ=10-60%) on the drawing process. A multidimensional forming quality evaluation system was established by introducing four quantitative indexes of geometrical characteristics, namely, fullerring coefficient (F), barrelling degree (B), maximum elongation ratio (E) and spread ratio (S). The orthogonal experimental design and full factorial combination method are used to construct a feature matrix containing 16 groups of process-response data, and a process parameter prediction model is developed by combining with the neural networks to realize the nonlinear mapping between the forming quality and the process conditions. The ultimate goal is to establish an accurate prediction model for the single-step drawing process and achieve multi-objective collaborative optimization.

Among them, four important parameters in the drawing process are the maximum elongation ratio (E), maximum spread ratio (S), barrelling degree (B) and reduction ratio (ξ), which are calculated using the following formulas:

$$E = \frac{l_1 - l_0}{l_0} \times 100\%, \tag{7}$$

$$S = \frac{W_{\max} - W_0}{W_0} \times 100\%, \tag{8}$$

$$\xi = \frac{h_1 - h}{h} \times 100\%, \tag{9}$$

where : l_0 - Length before forging, mm

l_1 - Length after forging, mm

h - Height before forging, mm

h_1 - Height after forging, mm

W_0 - Initial width of workpiece, mm

$W_{\max}$ - The maximum width of the workpiece after forging, mm

Due to the inevitability of friction, this article uses the barrelling degree (B) as one of the parameters to judge the shape of the workpiece after drawing. Zhang et al. [17] studied the causes and effects of drum formation during the flat anvil upsetting process, and gave the calculation formula for B:

$$B = \frac{W_{\max} - W_1}{W_1} \times 100\%, \tag{10}$$

where : $W_{\max}$ - The maximum width of the workpiece after forging, mm

W_1 - Spreading width of the contact surface with the anvil after forging, mm

In addition to considering the generation of “barrelling” shape, another important parameter to predict whether the workpiece meets the requirements after drawing is fullerring coefficient (F), which represents the ratio of the cross-sectional area before and after forging. The calculation formula of F is:

$$F = \frac{A_{after}}{A_{before}} \times 100\%, \tag{11}$$

$$A_{\text{after}} = \frac{1}{2}(W_{\max} + W_1) \times h_1, \tag{12}$$

where : A_{before} - Cross-sectional area before forging;

A_{after} - Cross-sectional area after forging.

6. Research results

Fig. 4 presents a comparison of results under different conditions of friction coefficient, pressing speed, and anvil temperature. It is evident from the figure that the friction coefficient and pressing speed have insignificant effects on parameters such as F, B, E, and S. However, the anvil temperature has a considerable impact on the S and B. Specifically, when the anvil temperature is low, the values of S and B increase. This phenomenon can be attributed to the “chilling” effect that occurs at the end face of the workpiece when the anvil temperature is much lower than the workpiece temperature. This “chilling” effect leads to an increase in material deformation resistance at the dead zone, thereby exacerbating deformation inhomogeneity. To avoid this unfavorable chilling effect, we should try to increase the anvil temperature. Therefore, in the subsequent analysis of the influence of b/h, w/h, and ξ on the drawing process, we will no longer consider the heat transfer between the anvil and the workpiece. That is, we assume that the forging process takes place under isothermal conditions. Under this premise, we set the pressing speed to 5mm/s and the friction factor to 0.3 to further simplify the analysis process and highlight the impact of key process parameters.

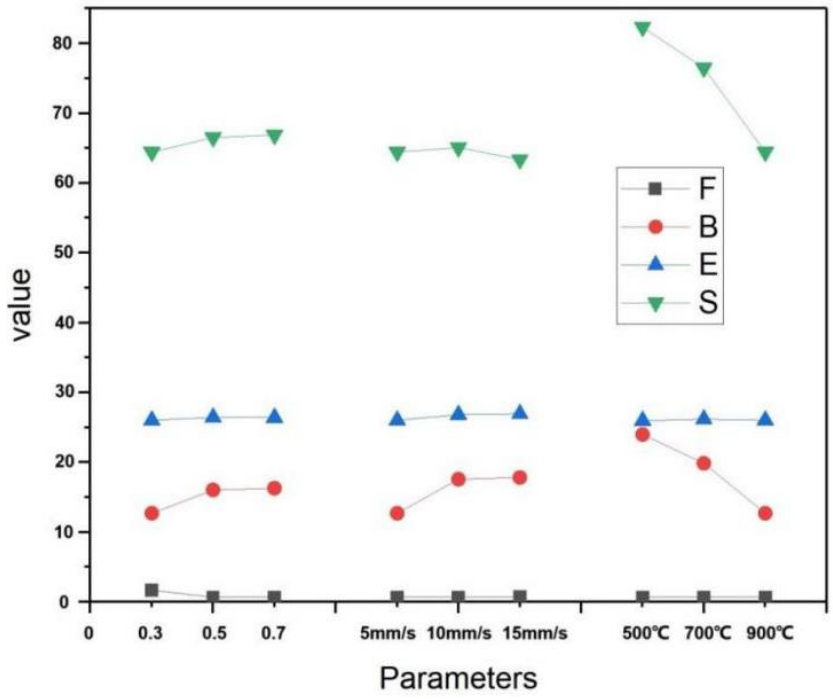

Figure 4. Comparison diagram under different friction coefficients, pressing speeds and anvil temperatures.

Fig. 5 shows a comparison of the effects of b/h, w/h, and ξ on F in a single step. Analysis reveals that F is directly proportional to the ξ and b/h, and inversely proportional to the w/h. When the ξ is below 20%, the increase rate of F is relatively moderate, and the influence of b/h and w/h on F is minor. However, when the ξ exceeds 20%, the growth rate of F becomes steep, and the impact of b/h and w/h on F becomes more significant. Additionally, it is worth noting that F is directly proportional to the w/h and inversely proportional to the b/h. Therefore, to achieve a higher value of F, it is necessary to maximize the b/h and ξ while minimizing w/h.

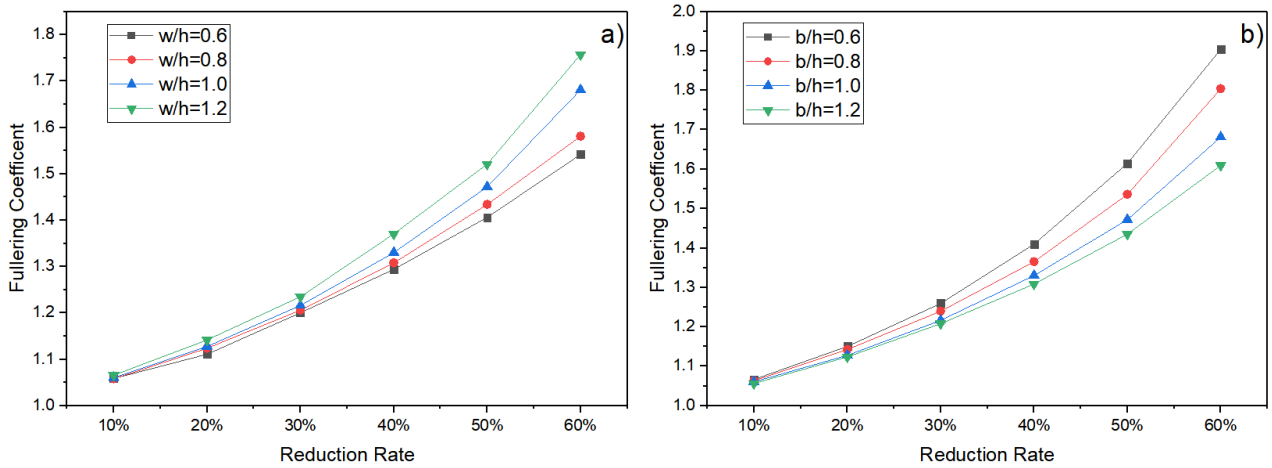

Figure 5. Comparison diagram of the effects of w/h, b/h, and ξ on F in single step (a - w/h vs F, b - b/h vs F).

Fig. 6 compares the effects of b/h, w/h and ξ on the B in a single step. Through in-depth analysis, we found that the B is directly proportional to the ξ and b/h, and inversely proportional to the w/h. Specifically, when the ξ is below 20%, the increase rate of B is relatively flat, and the influence of

b/h and w/h on B is not significant. However, when the ξ exceeds 20%, the growth rate of B accelerates significantly, and the impact of b/h and w/h on B also increases. Additionally, when the w/h is less than 0.6, there is an increased risk of double barreling, which is a critical aspect to consider during the design of the drawing process.

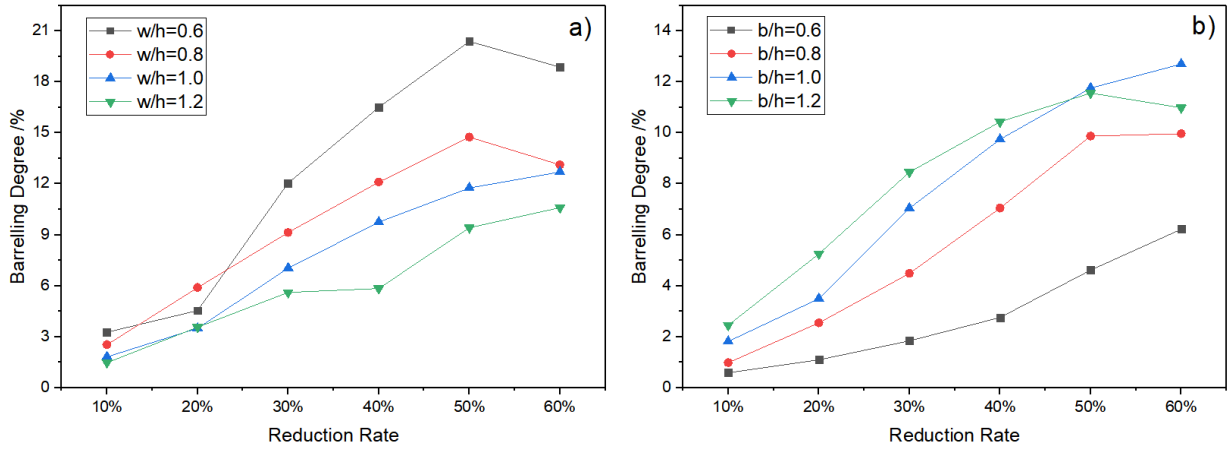

Figure 6. Comparison diagram of the effects of w/h, b/h, and ξ on B in single step (a - w/h vs B, b - b/h vs B).

Fig. 7 reveals the impact of b/h, w/h, and ξ on parameter E in a single step. It is evident from the figure that E is inversely proportional to the w/h and directly proportional to the b/h. This trend arises because as the w/h decreases or the b/h increases, the contact area between the anvil and the workpiece increases accordingly. Under the same ξ conditions, this increase in contact area leads to a larger amount of material transfer in the axial direction, which directly affects the value of parameter E. Therefore, in practical operations, we can adjust the w/h and b/h to control the axial flow of the material, thereby optimizing the quality and shape of the forging.

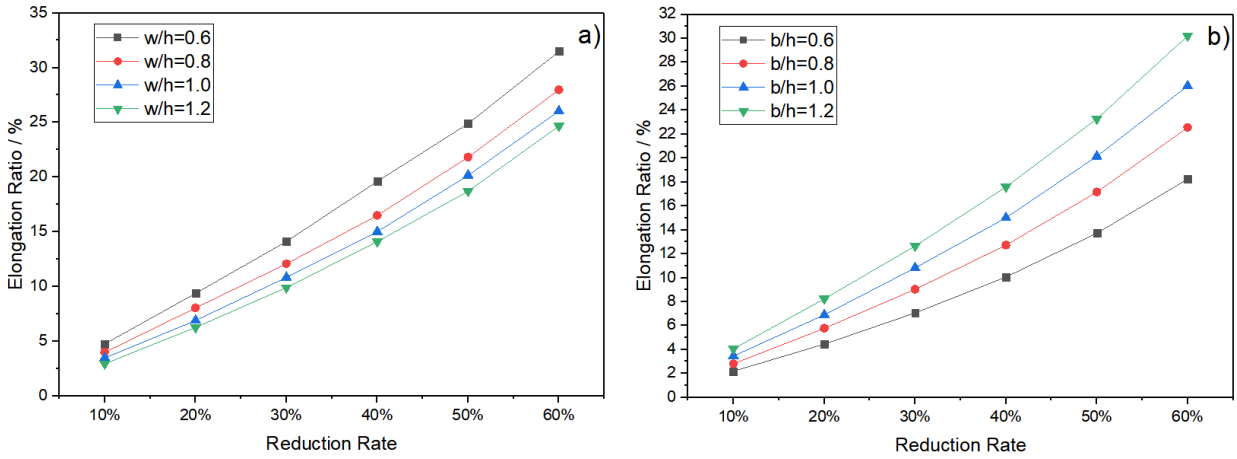

Figure 7. Comparison diagram of the effects of w/h, b/h, and ξ on E in single step (a - w/h vs E, b - b/h vs E).

Fig. 8 compares the effects of b/h, w/h, and ξ on S in a single step. As can be seen from the figure, the S is inversely proportional to the w/h and directly proportional to the b/h. The reason for this phenomenon lies in the unavoidable friction between the anvil and the workpiece. When the w/h decreases or the b/h increases, the dead zone at the contact point between the anvil and the workpiece enlarges accordingly. This increase in the dead zone promotes the tendency for barreling to occur, thereby affecting the variation in the S.

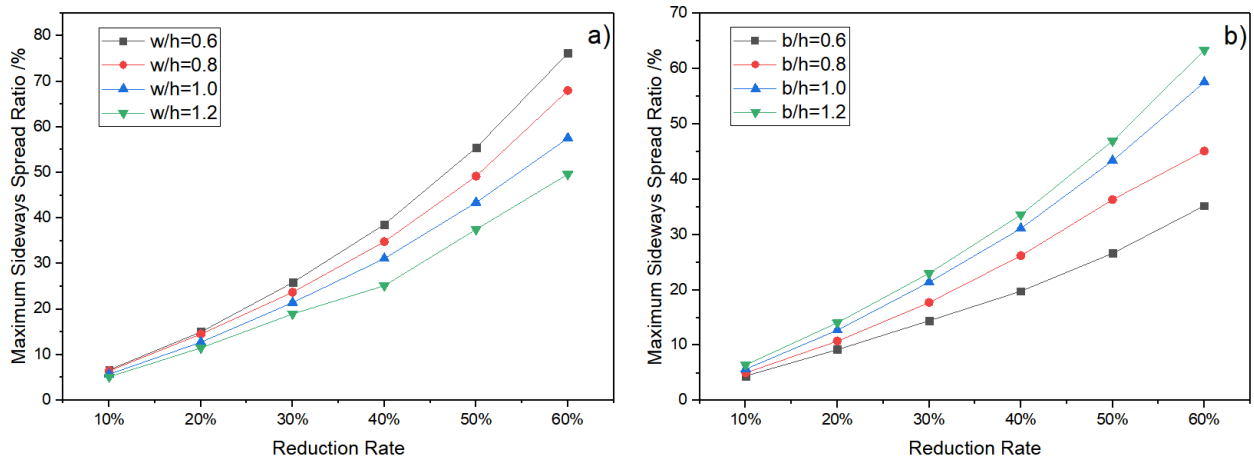

Figure 8. Comparison diagram of the effects of w/h, b/h, and ξ on S in single step (a - w/h vs S, b - b/h vs S).

Neural networks is an important branch in the field of machine learning, which simulates the structure and working mode of neural networks in the human brain. Neural networks are composed of a large number of neurons (or nodes) connected to each other. These neurons receive input signals and generate output signals through activation functions. During training, the network adjusts internal connection weights based on input data and desired outputs to minimize prediction errors[18][19]. Tab. 1 shows the sample data used for training learning which is obtained through finite element method(FEM).

Table 1. Sample data for training learning

No.	b/h	w/h	ξ /%	F	B/%
1	0.6	0.6	30	1.23	4.50
2	0.6	0.8	40	1.36	3.66
3	0.6	1	50	1.34	14.97
4	0.6	1.2	60	1.97	5.53
5	0.8	0.6	40	1.32	13.42
6	0.8	0.8	30	1.23	6.59
7	0.8	1	60	1.80	9.97
8	0.8	1.2	50	1.59	8.21
9	1	0.6	50	1.41	20.39
10	1	0.8	60	1.58	13.12
11	1	1	30	1.22	7.04
12	1	1.2	40	1.37	5.85
13	1.2	0.6	60	1.47	18.67
14	1.2	0.8	50	1.39	13.78
15	1.2	1	40	1.31	10.43
16	1.2	1.2	10	1.06	1.96

After rigorous training, verification and testing processes, the constructed neural network performed well in various evaluation indicators, especially the R value (correlation coefficient) was close to 1 during the training, verification and testing stages, as shown in Fig. 9. This result fully demonstrates that the neural network model can accurately fit the data and effectively extract useful information from the data.

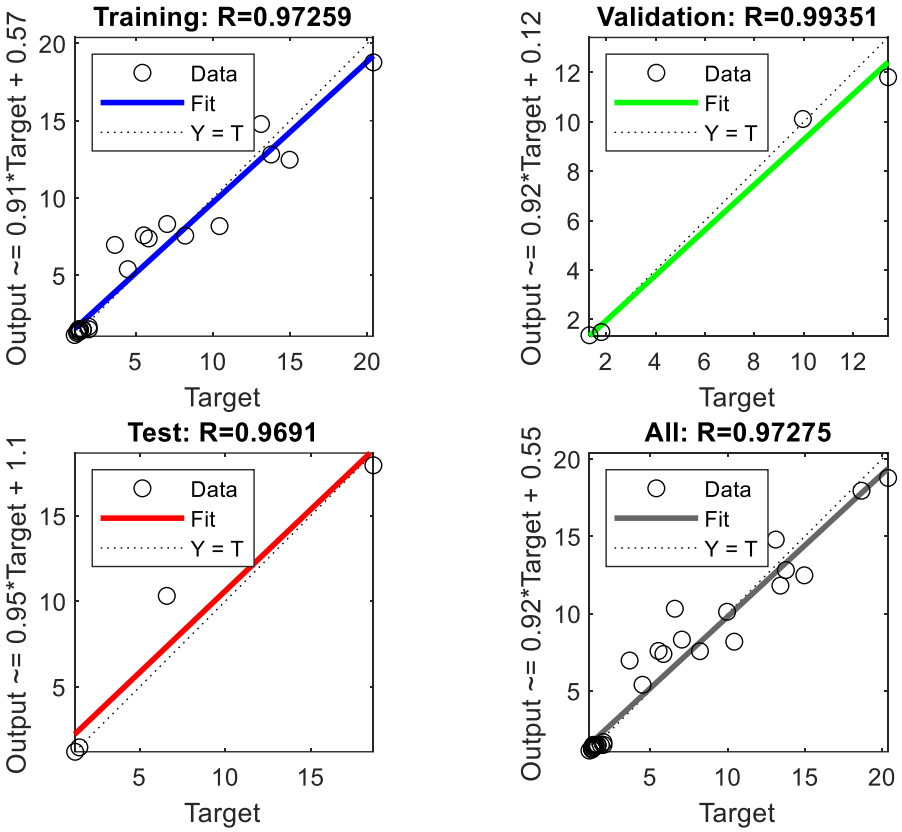

Figure 9. Regression of training, validation and test.

Tab. 2 presents a comparison between the predicted values from Neural network prediction model (NNP) and the simulated values from the finite element method(FEM). The data in the table reveals that the overall error remains within 2%, indicating a high accuracy of the established prediction model. However, under specific parameter combinations, such as an b/h=0.8, a w/h=8, and a ξ=50%, a maximum error of 12.54% is observed. 1) The sample data used to train the neural network is limited, and the computer may have certain limitations in understanding and learning material flow behavior. This can lead to larger prediction errors under specific parameter combinations. 2) The drawing process is a complex deformation process involving nonlinear material flow and coupling of multiple physical fields. Even if the neural network has learned a large amount of sample data, it is still difficult to accurately predict material flow behavior in all situations, resulting in prediction errors. Consequently, compared with the FEM, the NNP approach demonstrates superior computational efficiency, achieving high prediction accuracy with Limited sample size. This combination of reduced computational cost and data requirements substantially accelerates the design process.

Table 2. Comparative results of the NNP and FEM

No.	b/h	w/h	ξ /%	F		Difference/ %	B		Difference/ %
				NNP	FEM		NNP	FEM	
1	0.6	0.6	50	1.53	1.51	1.33	9.110	9.21	1.09
2	0.8	0.8	50	1.67	1.49	12.08	11.44	13.08	12.54
3	1.2	0.6	50	1.37	1.35	1.48	18.31	18.45	0.759

In the drawing process, the ξ is a crucial parameter. When the ξ reaches 50%, tensile stress starts to emerge at the transition between the loaded and unloaded zones. The occurrence of this tensile

stress may have adverse effects on the overall performance of the workpiece. In particular, when the ξ further increases to 60%, the area of tensile stress in the unloaded zone expands significantly. This situation greatly increases the risk of surface cracking and internal defects in the workpiece. Therefore, when designing the drawing process route, although increasing the ξ can improve drawing efficiency to some extent, it also increases deformation inhomogeneity. More importantly, we must fully consider the internal stress state of the workpiece. An excessively high reduction ratio may lead to uneven stress distribution inside the workpiece, thereby increasing the risk of damage.

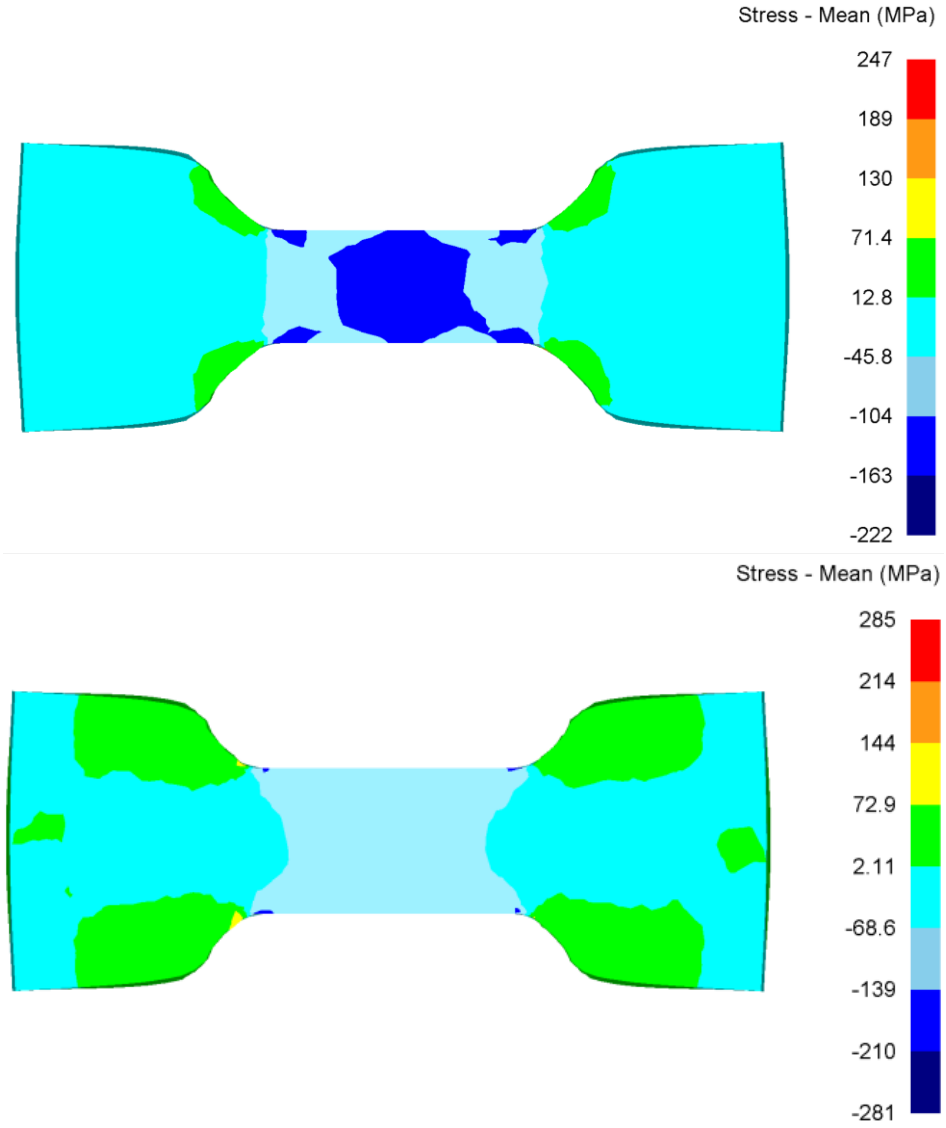

Figure 10. Stress distribution（a - ξ=50%, b - ξ=60%）.

To strike a balance between ensuring drawing process efficiency and guaranteeing the quality and safety of the workpiece, we conducted comprehensive considerations. Ultimately, this paper selects a reduction ratio ξ of 40% as a relatively ideal parameter. At this reduction ratio, the fullerring coefficient F remains between 1.3 and 1.4, resulting in a moderate barrelling degree B. Meanwhile, the elongation ratio E is maintained at a relatively high level, indicating that the workpiece can retain good deformation capability during the drawing process. To enhance the efficiency of the drawing process, this paper also adopts a single step per pass approach. Therefore, the anvil width needs to be longer than the elongation of the workpiece. After simulation, the final workpiece dimensions are shown in Fig. 11, with a calculated F value of 2.84. A higher F value means that the cross-section

ratio of the workpiece is larger, which can reduce unnecessary pre-forging process steps and improve production efficiency.

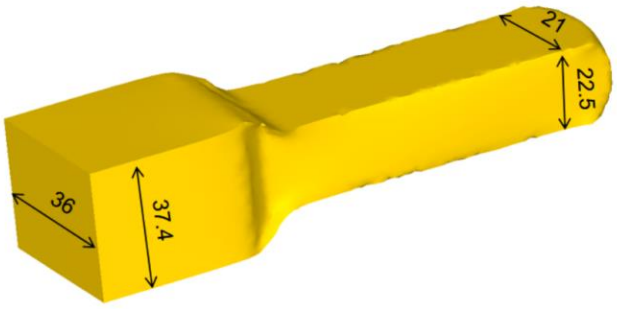

Figure 11. The workpiece after drawing process

7. Prospects for further research development

While this study successfully integrates thermomechanical-coupled FEM simulation and neural network modeling for process optimization of variable cross-section forgings, several avenues remain for future exploration. First, extending the methodology to multi-stage or multi-pass drawing processes could provide more comprehensive control over complex deformation paths and residual stress distribution. Second, integrating additional factors such as anisotropic material behavior, tool geometry, and real-time thermal gradients would further enhance model fidelity and practical applicability. Moreover, the use of advanced deep learning architectures (e.g., convolutional or graph neural networks) may improve prediction accuracy and generalization across different forging geometries.

8. Conclusions

This study built a quality prediction model for the drawing process by integrating finite element simulation and neural network technology. The thermomechanical coupling finite element analysis method was used to systematically reveal the coupling mechanism of six key process parameters on the drawing process, including temperature (500-900℃), friction factor (0.3-0.7), pressing speed (5-15 mm/s), anvil width ratio (b/h=0.6-1.2), width-height ratio (w/h=0.6-1.2) and reduction rate (ξ=10-60%). Four evaluation indicators(F, B, E, S) are introduced for the geometric characteristics of the workpiece after drawing. The study finally came to the following core conclusions:

1. Temperature, anvil width ratio (b/h), width-height ratio (w/h), and reduction ratio (ξ) are identified as dominant factors influencing the drawing process. A single-step reduction ratio of 40% is optimal for balancing efficiency and workpiece integrity, while exceeding 50% risks adverse internal stress states. Frictional effects and pressing speed exhibit negligible impact compared to these parameters.

2. A neural network framework is employed to analyze collected training data, establishing a high-precision predictive model with a post-training correlation coefficient of 0.973. Its robustness is further validated through rigorous testing across three independent datasets, demonstrating its capability to forecast deformation outcomes with high precision.

3. By analyzing the deformation characteristics of the single-step drawing process, a customized forming strategy was developed for the variable cross-section forgings. Through comparative analysis, the optimal process parameters were determined as follows: temperature of 900 °C, pressing speed of 5 mm/s, friction factor of 0.3, reduction ratio (ξ) of 40%, and a width-to-height ratio (w/h) of 1, anvil width ratio (b/h) of 1.2. Under these conditions, the maximum F value reached 2.84, the minimum B

value is 5.85%, providing strong technical support for Improving the production efficiency and quality of the variable cross-section forgings.

References:

1. Shutt, A. (1960). A note on spread in indenting. Applied Scientific Research, 9(1), 389.
2. Hill, R. O. D. N. E. Y. (1963). A general method of analysis for metal-working processes. Journal of the Mechanics and Physics of Solids, 11(5), 305-326.
3. Baraya, G. L. (1964). Flat Bar Forging and the Yield Criteria. The University of Manchester (United Kingdom).
4. Pahnke, H. J. (1983). Fundamentals of programmed forging. Metall. Plant Technol., 6(5), 92-101.
5. Tomlinson, A., & Stringer, J. D. (1959). Spread and elongation in flat tool forging. J. Iron Steel Inst, 193(2), 157-162.
6. Aksakal, B., Osman, F. H., & Bramley, A. N. (1997). Upper-bound analysis for the automation of open-die forging. Journal of materials processing technology, 71(2), 215-223.
7. Kudo, H. (1960). An upper-bound approach to plane-strain forging and extrusion—I. International Journal of Mechanical Sciences, 1(1), 57-83.
8. Baraya, G. L. , & Johnson, W. . (1964). Flat bar forging.
9. Sagar, R., & Juneja, B. L. (1979). An upper bound solution for flat tool forging taking into account the bulging of sides. International Journal of Machine Tool Design and Research, 19(4), 253-258.
10. Braun-Angott, P., & Berger, B. (1982). An upper bound approximation for spread and pressure in flat tool forging. Numerical Methods in Industrial Forming Processes, 165-174.
11. Kanacri, F., Lee, C. H., Beck, L. R., & Kobayashi, S. (1973). Plastic compression of rectangular blocks between two parallel platens. In Proceedings of the Thirteenth International Machine Tool Design and Research Conference (pp. 481-490). Macmillan Education UK.
12. Alexandrov, S., Lyamina, E., & Jeng, Y. R. (2023). Application of the upper bound theorem for metal forming processes considering an arbitrary isotropic pressure-independent yield criterion with no strength differential effect. The International Journal of Advanced Manufacturing Technology, 126(7), 3311-3321.
13. Mwema, F. M., & Obiko, J. (2021). Deformation behaviour of high-strength aluminium alloy during forging process using finite element method.
14. 丁艳宝. (2011). 厚板类锻件拔长的成形规律及应用研究 (Master's thesis, 中南大学).
15. Lee, S., Quagliato, L., Park, D., Kwon, I., Sun, J., & Kim, N. (2021). A new approach to preform design in metal forging processes based on the convolution neural network. Applied Sciences, 11(17), 7948.
16. Ilic, S., Karaman, A., Pöppelbaum, J., Reimann, J. N., Marré, M., & Schwung, A. (2024). Predicting Wall Thickness Changes in Cold Forging Processes: An Integrated FEM and Neural Network approach. arXiv preprint arXiv:2411.13366.
17. Zhang, X., Borysevych, V., & Chen, J. (2022). Selection of the rational geometry of specimen for compression test.
18. Schmidhuber, J. (2015). Deep learning in neural networks: An overview. Neural networks, 61, 85-117.
19. Arjun, K. S., & Aneesh, K. (2015). Modelling studies by application of artificial neural network using matlab. Journal of Engineering Science and Technology, 10(10), 1477-1486.